Atmos. Chem. Phys. Discuss., 9, 6657–6690, 2009
www.atmos-chem-phys-discuss.net/9/6657/2009/

Atmospheric Chemistry and Physics Discussions

This discussion paper is/has been under review for the journal *Atmospheric Chemistry and Physics (ACP)*. Please refer to the corresponding final paper in *ACP* if available.

Regional differences in organic composition of submicron and single particles during INTEX-B 2006

D. A. Day[1], S. Takahama[1], S. G. Gilardoni[1,*], and L. M. Russell[1]

[1]Scripps Inst. of Oceanography, University of California, San Diego, La Jolla, California, USA
[*]now at: European Commission, Institute for Environment and Sustainability, Ispra (VA), Italy

Received: 5 February 2009 – Accepted: 11 February 2009 – Published: 10 March 2009

Correspondence to: L. M. Russell (lmrussell@ucsd.edu)

Published by Copernicus Publications on behalf of the European Geosciences Union.

Abstract

Organic functional group and elemental concentrations were measured with Fourier transform infrared (FTIR) spectroscopy and X-ray fluorescence (XRF) from an aircraft platform as part of the Intercontinental Chemical Transport Experiment – Phase B (INTEX-B) conducted over the Eastern Pacific and Western North America. Single particle spectra were obtained using scanning transmission X-ray microscopy-near edge X-ray absorption fine structure spectrometry (STXM-NEXAFS). Organic mass (OM) concentrations ranged from 1 to 7 $\mu g\,m^{-3}$ and averaged 2.4–4.1 $\mu g\,m^{-3}$. Alkane functional groups were the largest fraction of OM, averaging 1.9–2.1 $\mu g\,m^{-3}$ or 50–76% of OM. Alcohol functional groups comprised the second largest fraction of OM (0.35–0.39 $\mu g\,m^{-3}$, 9–14%). Organic and elemental concentrations are compared within and among geographical air mass regions: "Pacific" free troposphere, "Continental" free troposphere, "Seattle" metropolitan region, and the California "Central Valley". OM concentrations were highest and most variable in the Central Valley (3.5±2 $\mu g\,m^{-3}$). Alcohol functional group concentrations were highest in the Continental and Central Valley and lowest in the Pacific and Seattle air masses. Oxygen-to-carbon ratios were relatively constant in the Central Valley but variable for the Continental air masses. Most elemental concentrations did not show large variations among or within air mass categories. Overall, the OM concentrations showed greater variability within air mass categories as compared to averages among them, suggesting sampled air mass regions included a variety of sources, processing, and losses of organic aerosol. Single particle spectra obtained by STXM-NEXAFS were classified into metaclasses associated with different sources and atmospheric processing. Particles with spectra indicative of secondary organic aerosol production and combustion sources were found at several locations and a range of altitudes. At lower altitudes, particles with spectra resembling soil dust and biomass burning fingerprints were commonly observed. Single particle spectra provided evidence that condensation and surface-limited oxidation contributed to particle growth.

ACPD

9, 6657–6690, 2009

1 Introduction

The organic fraction of submicron particles has been shown to be significant in nearly every region of the troposphere: urban (Zhang et al., 2005), rural (Alfarra et al., 2004), marine (Middlebrook et al., 1998), and the free troposphere (Novakov et al., 1997). Organic particles can enter the atmosphere directly though anthropogenic processes such as fossil fuel combustion and biomass burning or natural pathways such as wind-driven dust and soil suspension. Despite the recognition of the ubiquity of organic aerosol in the atmosphere, the organic composition is largely uncharacterized, in part due to the large number of chemicals involved (Lewis et al., 2000) and the analytical challenges associated with this heterogeneity (Turpin et al., 2001).

The free troposphere is an under-sampled part of the atmosphere, primarily due to the limitations of conducting aircraft measurements. The Intercontinental Chemical Transport Experiment – Phase B (INTEX-B) campaign was designed to investigate one of these regions, the free troposphere above the Eastern Pacific and Western North America. The primary goal of INTEX-B was to gain understanding of transport and evolution of Asian pollution and how it impacts air quality and climate in Western North America (Singh et al., 2009). There are very few measurements of organic aerosol composition in the free troposphere over the Pacific between the Asian and North American continents, and an even larger gap in the understanding of the export of organic aerosol from Asia and trans-Pacific transport and processing. For example, models have been shown to under-predict organic carbon in the free troposphere over the Northwest Pacific by 1–2 orders of magnitude (Chung and Seinfeld, 2002; Heald et al., 2005). Understanding these discrepancies is vital to quantifying the impact that Asian pollution may have on North American air quality.

In this manuscript, we present measurements of organic functional groups and elemental composition of submicron particles collected as part of the INTEX-B study. Since many of the air masses sampled in the free troposphere included a variety of sources in addition to Asian pollution, we focus our discussion on characterizing dif-

ferences in organic composition between and within geographically-defined air mass regions, namely the Northeastern Pacific free troposphere, the Western North American free troposphere, the Seattle metropolitan region, and the California Central Valley. The organic functional group quantification was achieved using Fourier transform infrared (FTIR) spectroscopy. Single particle measurements were also obtained using scanning transmission X-ray microscopy – near edge X-ray absorption fine structure spectrometry (STXM-NEXAFS), allowing classification of particles into metaclasses indicative of general sources and atmospheric processing.

2 Experimental methods

2.1 Sample collection

Aerosol measurements discussed in this manuscript were collected during the Intercontinental Chemical Transport Experiment – Phase B (INTEX-B) from the NCAR C130 aircraft during April and May 2006. The aircraft was based at Paine Field in Everett, Washington, just north of Seattle. Twelve flights were conducted, all based at Paine field except the transit fights bracketing the study between Colorado and Washington. Flight tracks are available at: http://www-air.larc.nasa.gov/missions/intex-b/images/thumbnailmaps_c130_IMPEX.pdf. The majority of the flight time was in the free troposphere above the Eastern Pacific or Western Washington, Oregon, and California with the primary goal to intercept pollution layers transported from Asia. In addition to profiles of the free troposphere, some flights included legs in and just above the boundary layer over the Pacific Ocean, Seattle metropolitan area, and the California Central Valley.

From a common inlet, 16.7 ambient L min^{-1} was sampled, with the mass flow rate varying inversely with altitude. Sample air passed through a PM_1 cyclone to select for submicron particles. The sample flow was split, and aerosol particles were collected on two sets of duplicate 37 mm diameter Teflon filters. Particles were collected contin-

ACPD
9, 6657–6690, 2009

uously on one filter set for the duration of each flight (as a backup). The other "short" samples were collected on several different filters that were sampled for periods ranging from ~5 min to ~1 h, with resulting total flow volumes of 0.02 to 0.3 m^3. Typically these "short" samples were in place for the duration of a level flight leg. Teflon filters were stored in polystyrene Petri dishes, sealed with Teflon tape, and kept at −4°C for later analysis. A total of 76 "short" samples were collected during the 2 transit and 10 research flights of this study.

In addition to the submicron filter samples collected for quantitative mass-based analysis, particles for single particle analysis were collected on Si_3N_4 windows (Silson Ltd.) that were mounted on a rotating impactor (Streaker, PIXE International, Inc.). One standard L min^{-1} (SLM) of air was drawn through Al tubing to the impactor. Samples were frozen after collection until time of analysis.

2.2 Organic and Elemental Analysis

FTIR spectroscopy was used to quantify organic functional group concentrations for the particles collected on each Teflon filter. Detailed descriptions of the method can be found in Maria et al. (2002, 2003) and Gilardoni et al. (2007). Revisions to those method descriptions include use of an automated algorithm for baselining, peak fitting, and integration and additional calibrations of primary amine and carboxylic acid functional groups (Liu et al., 2009; Russell et al., 2009). Functional groups quantified include: saturated aliphatic (hereafter alkane) groups, unsaturated aliphatic (hereafter alkene) groups, aromatic groups, alcohol groups (including phenols), carboxylic acid groups, non-acidic carbonyl groups, primary amine groups, and organosulfate groups. Due to a combination of generally low organic aerosol concentrations and the limited sampling intervals dictated by the short flight legs, only 17 "short" samples contained organic functional groups above the detection limits required for total organic mass (OM) quantification. Alkene, aromatic, amine, and organosulfate groups were below detection limit for all samples, with alkene and aromatic functional groups accounting for 4% and 3% of OM, respectively. The spectra were analyzed for evidence of

organosulfate functional groups at 876 cm^{-1} but no detectable absorption peaks were identified in any samples. For most samples discussed in this manuscript, carboxylic acid groups were also below the detection limit, in part due to the water vapor absorption features in pre-scanned blank filters in the 1600–1800 cm^{-1} region. Water vapor interference resulted in the inability to quantify primary amine functional groups using the absorption peak at 1625 cm^{-1}. We estimate that they could have accounted for at most 10% of OM. This study reports only alkane, alcohol, and carboxylic acid functional groups as they typically constitute the majority of OM. Concentrations of carboxylic acid groups were calculated as the molar carbonyl concentrations.

Several samples were not excluded from this analysis when some of the major three functional groups did not meet our typical signal-to-noise >2 detection limit criteria. Therefore we estimate upper bounds for functional group concentrations by assigning below detection limit (BDL) functional groups to the detection limit (DL) concentrations. For much of the discussion that follows, we express the organic composition as ranges bounded by the measurements and the upper limit. We consider these limits to be a more accurate representation of our FTIR observations, particularly when contrasting regional averages. Unless otherwise indicated, throughout this manuscript reported ranges represent these limits, whereas single numbers and mean ± standard deviation (expressing variability) indicate actual measurements.

We compared the OM observed with FTIR measurements to measurements of OM also made on board the C130 with an Aerodyne High Resolution Time-of-Flight Aerosol Mass Spectrometer (HR-ToF-AMS) (Dunlea et al., 2008). The average magnitude of OM concentrations during overlapping sampling periods compared well, although the variability and small dynamic range of the measurements resulted in several points exceeding the expected ±20–25% error of each instrument. At the lowest concentrations, FTIR OM tended to be somewhat higher than that measured by the HR-ToF-AMS. We also compared the O/C ratios calculated from the FTIR functional group concentrations to the O/C ratios calculated using the HR-ToF-AMS *m/z* 44 and total organic mass concentrations according to the relationship discussed in Aiken et al. (2008).

ACPD
9, 6657–6690, 2009

General agreement was observed within the uncertainties for the FTIR measurements discussed in Sect. 3.1 and that for the AMS measurements (±30%).

X-ray fluorescence (XRF) measurements (Chester LabNet, Tigard, Oregon) of submicron particles were conducted using the same filters as used for the FTIR analysis to quantify elemental concentrations heavier than Na (Maria et al., 2003). Approximately half of the filters (47) were selected for XRF analysis, in part, by the presence of detectable organics. Of these samples, 40 had at least one element that was reported as above the detection limit (defined as a signal-to-noise ratio of two); however, only ten samples had more than ten elements above the detection limit. All organic and elemental concentrations reported here are in units of $\mu g\,m^{-3}$ air at STP.

Single particles collected on the Si_3N_4 windows were analyzed at the Advanced Light Source at the Lawrence Berkeley National Laboratory (Berkeley, CA) using STXM-NEXAFS. Transmission of photons at energy levels between 278 and 320 eV was measured over a minimum spatial resolution of 30 nm and converted to optical density using a protocol described by Russell et al. (2002). Spectra were then classified according to the presence and relative absorbance intensities of organic functional groups (alkyl, ketonic, carboxylic carbonyl, alkene, and aromatic), carbonate, and potassium. Particles were also categorized as having a "spherical" or "irregular" morphology. Details of the spectral and image classification methods are described in Takahama et al. (2007). Takahama et al. (2007) analyzed ~600 single particles collected at several locations and identified 14 spectral categories.

For this study, 113 particle spectra were obtained from 10 locations. Each of the spectra from the individual particles were classified into categories established by Takahama et al. (2007) both by manual means and according to the *k*-nearest neighbor algorithm (which used 25% of the spectra from Takahama et al. (2007) in each category that most closely resembled the "average" spectra as the training dataset). The size reported is the geometric diameter for the 17 particles analyzed by Takahama et al. (2007), and sphere-equivalent diameter of the 2-D image projection for the additional particles analyzed in this study.

ACPD
9, 6657–6690, 2009

The STXM-NEXAFS spectra were also analyzed to determine quantitative surrogates for the total mass, total carbon mass, and carboxylic carbonyl content of individual particles as described by Maria et al. (2004). The absorbance associated with carboxylic carbonyl (288.7±0.3 eV) was integrated simultaneously with a Gaussian peak and the underlying K-edge step-like absorbance with an arctan function as described in Takahama et al. (2007). The absorbance at 278–283 eV is integrated as absorbances of inorganic species, and the elevated absorbance in the 305–320 eV region is attributed to the total carbon (Maria et al., 2004). The ratios of these absorbances were converted to absolute mass ratios using concurrent bulk submicrometer particle measurements: carboxylic acid functional group and organic carbon concentrations measured by FTIR and total mass concentrations measured by AMS. This conversion yielded total carbon-to-total mass ratios, carboxylic carbonyl carbon-to-total mass ratios, and carboxylic carbonyl carbon-to-carbon ratios for each particle (Maria et al., 2004).

2.3 Air Mass Categorization

The diversity of flight locations allowed for sampling of a wide range of different air masses, likely affected by varying sources and degrees of processing. Therefore, as a framework for much of the discussion presented here, the observations have been divided into different air masses, primarily by geographic criteria. Dunlea et al. (2008) present aerosol measurements from the INTEX-B campaign and define four air masses based on a combination of geographic and chemical factors. Namely, they separate air into "Asian pollution layers," "free troposphere," "Central Valley," and "Seattle". "Asian pollution layers" and "free troposphere" are defined as air sampled west of −125 longitude, over the Pacific Ocean, and above the marine boundary layer. They are separated by sulfate loading greater or less than 1 μg S m^{-3}, respectively. "Seattle" included most of flight 3, conducted largely in the Seattle region above the planetary boundary layer. "Central Valley" air masses included two low altitude passes within the California Central Valley boundary layer during flight 7. For our analysis, we expand the "Central

ACPD
9, 6657–6690, 2009

Valley" category to include additional legs from flights 9 and 11 when the aircraft flew at ~500 m in the Central Valley. Similarly, we include an additional sample collected in the Seattle region on a different flight (flight 10), but exclude a sample collected at ~5000 m during the "Seattle flight". The distinction of Asian and free tropospheric air mass was not used since many of the filters collected over the Pacific contained a mixture of both "Asian pollution layers" and "free troposphere" air masses, since the criteria of Dunlea et al. (2008) required shorter sampling durations than were available for in-flight filter collection. Measurements collected above the boundary layer and not classified as "Seattle" or "Central Valley" are split into those collected above the "Pacific" and above the North American continent ("Continental"). Figure 1 shows the locations of the constant altitude samples collected for FTIR, XRF, and STXM-NEXAFS analyses.

3 Results

3.1 FTIR Organic Composition

Table 1 summarizes the FTIR measurements. Campaign averages of OM and OC concentrations were 2.4–4.1 $\mu g\,m^{-3}$ and 1.8–2.4 $\mu g\,m^{-3}$, respectively. Alkane functional group concentrations were nearly always the largest fraction of OM, averaging 1.9–2.1 $\mu g\,m^{-3}$ or 50–76% of OM. Alcohol functional groups were 0.35–0.39 $\mu g\,m^{-3}$ and comprised 9–14% of OM. Carboxylic acid functional groups were 0.2–1.6 $\mu g\,m^{-3}$ comprising 10–40% of OM. Campaign averages of organic-mass-to-organic-carbon ratios (OM/OC) and oxygen-to-carbon (O/C) were 1.6–1.8 and 0.3–0.5, respectively.

3.1.1 Regional Differences in Organic Composition

Organic functional group concentrations are shown in Fig. 2 and are grouped by the research flight with the associated air mass category (as defined in Sect. 2.3) indicated. OM concentrations ranged from 0.8 $\mu g\,m^{-3}$ in a Continental sample to 6.5 $\mu g\,m^{-3}$ for a

ACPD
9, 6657–6690, 2009

Central Valley sample. OM was highly variable for the Central Valley, Continental, and Pacific samples. Seattle air mass samples consistently showed lower concentrations, all between 1 and 2 $\mu g\,m^{-3}$. Alcohol concentrations varied by more than an order of magnitude and generally did not track OM concentrations except for a few of the highest OM observations. Also shown in Fig. 2 is the time series of the O/C ratios and the relative contributions from the two oxygenated functional groups. Like alcohol functional group concentrations, O/C spanned more than an order of magnitude.

Organic functional group concentrations, OM, fractions of OM, and OM/OC and O/C ratios, grouped by air mass category, are shown in Fig. 3. Upper and lower bounds as defined in Sect. 3.1 are shown for each air mass – component combination (ranges of the means for each air mass are also shown in Table 1). Mean OM concentrations were: 2.2–4.5 $\mu g\,m^{-3}$ for Continental; 3.4–4.5 $\mu g\,m^{-3}$ for the Central Valley; 2.6–3.9 $\mu g\,m^{-3}$ for Pacific; and 1.4–3.1 $\mu g\,m^{-3}$ for Seattle, indicating that OM concentrations were the highest for the Central Valley, the lowest for Seattle, and the Continental and Pacific samples were indistinguishable. Alcohol functional group concentrations were highest for the Continental (0.46–0.51 $\mu g\,m^{-3}$) and the Central Valley (0.49 $\mu g\,m^{-3}$) and lowest for the Pacific (0.16–0.24 $\mu g\,m^{-3}$) and Seattle (0.16–0.24 $\mu g\,m^{-3}$) air masses. Measured carboxylic acid groups were a large fraction of OM for three Continental samples (30–50%). The alkane groups, as a fraction of OM, showed some regional differences with Pacific the highest (59–93%), followed by Seattle (44–85%), the Central Valley (55–76%), and Continental (43–61%). There may have been significantly higher average alkane fractions in the Pacific air masses relative to the Continental.

Since alkane groups were the only non-oxygenated group detected, the OM/OC and O/C are roughly the mirror images of the alkane group fraction. For the Pacific and Seattle categories, OM/OC and O/C are omitted in Fig. 3b and Table 1 since the sample loadings were too low to provide reasonable bounds on the measured range. For the Continental and Central Valley samples, average O/C ratios were 0.4–0.6 and 0.2–0.4, respectively, indicating that Central Valley O/C was lower than Continental samples. Observed O/C ratios showed a much larger variability in Continental air masses

ACPD
9, 6657–6690, 2009

(0.38±0.28) than the Central Valley (0.18±0.04).

3.1.2 Trends with Altitude in Organic Composition

In addition to the broad geographic extent of sample collection, a wide range of altitudes were sampled. We consider here the relationships of submicron organic particle composition with altitude. Figure 4 displays the organic functional group measurements in relation to altitude. There were few discernable trends with altitude. The OM concentrations were highest and most variable below 1000 m. A large fraction of the lower altitude samples were collected in the Central Valley and Seattle air masses, so that the altitude trend reflects in part a geographic sampling bias. Figure 4 shows that the average O/C of 0.4–0.6 observed for the Continental samples extended over a large vertical range (1800–6000 m), whereas the average O/C of 0.2–0.4 for the Central Valley was for samples collected at low altitude (<600 m), contained within the continental boundary layer (boundary layer height ∼1000 m).

Measurements conducted concurrently with the HR-ToF-AMS, revealed no distinguishable vertical trends in OM other than an enhancement in the Central Valley and at ∼6000 m in "Asian pollution layers" sampled during a single research flight (Dunlea et al., 2008). Similarly, measurements conducted in a region closer to large organic emission sources during ACE-Asia over the NW Pacific between 2–6.5 km showed very little vertical gradient (Heald et al., 2005).

3.1.3 FTIR Spectra Clustering Analysis

We applied agglomerative hierarchical clustering with the Ward algorithm to the FTIR spectra to identify similarities among spectra, possibly indicative of similar organic composition or sources and processing. FTIR spectra were normalized by the maximum absorbance peak. This analysis identified five distinct cluster groups. The principal difference among the cluster averages appeared to be the relative intensities of the broad absorbance peaks at 3150–3300 cm^{-1} (alcohol groups and ammonium) and 2900–

ACPD
9, 6657–6690, 2009

3100 cm^{-1} (alkane groups and other unidentified peaks). Groups 1 and 3 spectra, into which more than half of the spectra were grouped, are similar to three cluster averages identified by Liu et al. (2009) (numbers 5–7), who compared FTIR spectra from two ground sites and one airborne platform in Mexico.

Group 1 was the dominant group, containing one third of the spectra. It contained spectra from all air masses and had a wide range of OM concentrations (actual: 1.1–6.5 $\mu g\,m^{-3}$) and O/C ratios (actual: 0.03–0.28). Pacific air mass samples favored this category, and the three samples associated with this group showed the highest OM of the Pacific air mass category. All samples within Group 3 exhibited below average OM and O/C, the former of which may be related to the similarity of its shape to that of ammonium absorbance. Group 5 was composed of only Continental samples. These two samples contained the highest O/C ratios of all samples (0.70–0.82, 0.51–0.70): one with typical OM concentration (2.0–3.6 $\mu g\,m^{-3}$), and the other with low OM concentration (0.8–2.3 $\mu g\,m^{-3}$).

3.2 Elemental Composition

Trace element composition of aerosol particles can be used to obtain qualitative and quantitative information about particle sources (Miranda et al., 1996; Johnson et al., 2008; Gilardoni et al., 2009; Liu et al., 2009; Russell et al., 2009). We focus here on geographic and vertical trends of the elemental components of submicron particles. Elements and mean concentrations that were observed to be above the detection limit for at least ten samples with XRF analysis were (ng m^{-3}): Al (170), Si (230), S (250), K (47), Ca (76), V (25), Fe (48), Zn (44), Sn (210), and Ba (71). Median concentrations were generally 10–35% lower. Compared to measurements made on the same aircraft in Mexico prior to this study (Liu et al., 2009), these average concentration are all within a factor of 2–3.

Trace metal concentrations are shown in Table 1 separated by air mass categories. Few significant trends were observed with air mass classification. On average, Fe and

ACPD
9, 6657–6690, 2009

Zn had the lowest concentrations in the Central Valley compared to the other three air mass categories sampled. Whereas both Fe and Zn contained in aerosol may result from industrial processes, Fe may also result from soil and dust suspension (Johnson et al., 2006). The higher and more variable concentrations of these elements observed in the Pacific and Continental air masses are likely the result of much more varied sources, possibly substantially influenced by Asian transport compared to a more homogenous and geographically smaller Central Valley. Other notable observations are the particularly high concentrations of Al, Si, V, K, and Ca for a few samples. The highest K concentration observed (170 ng m^{-3}), approximately four times the campaign average, was for a sample collected in the Central Valley. Elevated potassium is commonly attributed to biomass burning and soil particles (Malm et al., 1994). For an earlier flight in this campaign within the Central Valley, Dunlea et al. (2008) report short, elevated HCN plumes, a strong indicator of biomass burning. Overall, most elemental concentrations were very similar within and among the different air mass categories.

The variation of elemental concentrations with altitude are shown in Fig. 4. Elevated (and more variable) concentrations of Ca, Ba, and Zn were observed at higher altitude. Two samples with high Al and Si concentrations (above 500 ng m^{-3}) were observed at high altitude, possibly indicative of mineral dust transported from Asia. Concentrations of Al and Si of an order of magnitude higher have been observed for submicron aerosol over the Western Pacific and attributed to mineral dust from Asian deserts (Maria et al., 2003). Both of these samples also had the two largest concentrations of Sn and V observed in this study. The sample collected at 6800 m above the Pacific, had the highest Ni, Ba, Mg, and Zn concentrations observed. Although elevated elemental concentrations in these samples may be indicative of transported Asian pollution, they appear to contain a mixture of tracers commonly associated with dust (Al, Si, Mg, Sn), oil combustion (Ni, V), and industry (Zn) (Johnson et al., 2006). Both of these samples were collected during periods thatMcKendry et al. (2008) identified as high aerosol episodes at Whistler Peak in British Columbia (2180 m), attributed to dust storm events from Northeast Asia. We also note that the highest Ca concentration ob-

served (390 ng m^{-3}) was collected near Seattle and coincided with the same day that the highest Ca concentration was observed (140 ng m^{-3}) at Whistler peak (McKendry et al., 2008).

Figure 4 also shows that sulfur had a weak negative correlation with altitude, indicating marine (for the Pacific region) or North American (for the Seattle, Continental, and Central Valley) boundary layer sources. Heald et al. (2005) observed a strong vertical gradient in the lower 4 km of the atmosphere over the Eastern Pacific associated with continental emissions. Gradients in non-sea salt sulfate have been observed over the Pacific Ocean extending above the MBL into the free troposphere, attributed to oxidation products of dimethylsulfide (DMS), a biogenic gas emitted from the Ocean (Dibb et al., 1999).

Dunlea et al. (2008) report that negative gradients with altitude were observed for the Seattle and Pacific regions in the lower 1 km and for the lower 2 km for the Central Valley region. In contrast, the air masses they identified as "Asian pollution layers" showed a positive gradient with altitude for 0 to 6 km. Using observations obtained with PILS-IC, also collected onboard the C130, Peltier et al. (2008) show an average gradient in sulfate between <3 km (~0.8 μg m^{-3}) and >3 km (~0.4 μg m^{-3}) for air masses they identified as influenced by North American air masses (using FLEXPART carbon monoxide). This gradient is similar to that shown in Fig. 4.

A few weak (r>0.25) to moderate (r>0.5) correlations between organic composition and elemental concentrations in submicron particles were observed. OM showed positive trends with Al, Si, S, V, and Sn (r=0.4–0.8). Additionally, O/C had negative correlations with Si and S (r= – 0.4) and positive correlations with Zn and Sn (r=0.5–0.8). OM and trace metals are expected to correlate since for most sources of trace metals, organic aerosol or organic aerosol precursors are co-emitted.

3.3 Single Particle Spectra Analysis with STXM-NEXAFS

The morphology and carbon K-edge signature of 113 individual particles were examined by STXM-NEXAFS. Forty-percent of particles analyzed were associated with Continental, 45% from Pacific, and 15% from Seattle air masses. The particles examined ranged between 0.26 and 30 μm (Figs. 5 and 6), 42% of the particles analyzed were between 0.1 and 1.0 μm (Fig. 6) and included both spherical and irregular morphologies (Fig. 5). Spectral analysis and subsequent classifications indicated similarity to a large number of established categories (Takahama et al., 2007) for all air mass regions. As the penetration depth of the NEXAFS beam is approximately 1 μm of pure carbon (Braun, 2005), the spectra for supermicron particles typically included those regions for which the particle is optically thin (i.e. near the edges) where the signal is not saturated. Several spectra categories in Fig. 5 belong to one of four metaclasses – Secondary, Biomass, Ultisol, and Combustion, determined by similarity to spectra of samples with known composition in the published literature. Fifteen particles with type "f" spectra (Ultisol), 28 Secondary, 26 Combustion, and 17 Biomass particles were found over a wide range of sizes (Fig. 6).

Several features of the STXM-NEXAFS single particle analysis illustrated in Figs. 5 and 6 indicate the composition and sources of particles observed in this study and their variability with location and altitude. Type "a" particles (which constitute the Secondary metaclass) associated with a strong carboxylic carbonyl signature (288.7±0.3 eV) and likely indicative of biogenic or other secondary organic aerosol, were the most common type observed. Several of these particles were Pacific samples, suggesting that Pacific samples may have contained significant fractions of carboxylic acid functional groups (and high O/C) in supermicron particles which were not sampled for FTIR. Types "i" and "j" spectra (which are part of the Biomass metaclass) have multiple functional group absorbance peaks, which may be associated with biomass burning. Several particles were observed that were classified into this Biomass category (most at lower altitudes) suggesting that long-range transport of Biomass aerosol was not common

ACPD
9, 6657–6690, 2009

for these observations.

The most common combustion-type particles (identified by a strong aromatic absorbance at 285.0±0.2 eV) observed was type "d". This particle type was also previously observed in samples collected on an aircraft during ACE-Asia and MILAGRO (Takahama et al., 2007). Note that many of the particle types in the Combustion metaclass are >1μm (b, d, h). This chemical signature is associated with "primary" or "emitted" particles, those emitted directly from combustion sources or formed rapidly thereafter. This association of combustion-type organics with larger particles could be due to coagulation with dust. Leaitch et al. (2008) argued that the presence of organics on coarse particles (for a subset of this STXM dataset) supported their hypothesis that scavenging of secondary organic aerosol (SOA) precursors by dust was responsible for observations of decreased concentrations of fine particle organic mass for higher loadings of supermicron dust particles.

The observation of several type "f" or Ultisol particles (in four separate samples) was a surprising result as previous instances of this unusual spectral type in a study of ~600 particles occurred only in those collected over the Caribbean Ocean (Takahama et al., 2007); reference spectra resembling this type was pine Ultisol soil from Puerto Rico (Ade and Urquhart, 2002). The relative prevalence at lower altitudes is consistent with more regional soil dust or biomass burning sources. Type "k" was one of the most frequently observed particle types, found at a range of altitudes and air masses. This particle type is not assigned to any metaclass because of the absence of distinct spectral features and lack of resemblance to any known standard. Many particle types of "a", "d", "i", and "k" were analyzed in Continental and Pacific samples (especially those aloft), collected over the broad INTEX-B region of the Western US and Eastern Pacific. We observed these groups with high frequency during ACE-ASIA (except for "d"), showing similarities between particles in the Northeastern and Northwestern Pacific that provide further support for long-range transport as an important source.

Results from the quantitative analysis of absorbance ratios using STXM-NEXAFS spectra discussed in Sect. 2.2 are shown in Fig. 7. Panel a shows the total carbon-to-

total mass of the particle. Panel b shows the carboxylic carbonyl carbon-to-total mass ratio. Finally, panel c shows the carboxylic carbonyl carbon-to-carbon ratio. Ratios are shown as a function of particle size in order to investigate relationships that may provide evidence for different particle growth and oxidation processes as described by Maria et al. (2004). Figure 7 includes only particles that were classified as type "a" (Secondary). All three ratios increase with decreasing particle size. According to the scheme presented by Maria et al. (2004), the size dependence in the total carbon-to-total mass ratio (panel a) indicates SOA formation by condensation or surface reaction. Furthermore, the size dependence of the carboxylic carbonyl carbon-to-total mass ratio (panel b) suggests that the organic compounds were oxidized. Finally, the size dependence of the carboxylic carbonyl carbon-to-carbon ratio (panel c) suggests that the oxidation processes were surface-limited. No individual sample analyzed with STXM-NEXAFS or any one air mass region had sufficient ranges in particle sizes to investigate the relationships shown in Fig. 7. Therefore, we cannot attribute the evidence for the condensation/surface-limited oxidation to one particular air mass or region but instead suggest this process was collectively important in the growth of Secondary particles (collected primarily in Pacific and Continental air masses).

4 Discussion

We compare our FTIR measurements for different air mass regions to other relevant observations. Gilardoni et al. (2009) report organic aerosol compositions for measurements made from aircraft in Mexico. They report average OM concentrations of 5.4 $\mu g\,m^{-3}$ that represents a mixture of samples collected in the Mexico City metropolitan area boundary layer and outside the city, often in the free troposphere. This average OM concentration is significantly higher than all of the air mass averages in this study, but most similar to the concentrations observed in the Central Valley (3.4–4.5 $\mu g\,m^{-3}$). The relative fractions of alcohol and alkane groups for that study (averages: 17–21%, 48–59%) are similar to the average fractions we observe for the Continental (10–19%,

43–61%) and Central Valley (12–16%, 55–76%) sectors. Low-altitude aircraft measurements in plumes over Ohio during ICARTT 2004 (Gilardoni et al., 2007) included average OM concentrations of 4.6 $\mu g\,m^{-3}$, at the high end of the Continental air masses concentrations discussed here (2.2–4.5 $\mu g\,m^{-3}$) and similar to Central Valley concentrations. The alkane and alcohol group contributions to OM for that study were also comparable to the Central Valley averages, at 22% and 64%, respectively.

There are no published measurements of organic functional group composition in Northeast Pacific air masses. Maria et al. (2003) report measurements of organic functional groups in submicron particles over the Northwest Pacific during the ACE-Asia campaign. Approximately, half of their samples were collected in the free troposphere and OM concentrations spanned from 0.6 to 19.6 $\mu g\,m^{-3}$. They report functional group fractions of OM and OM/OC as averages for ten "back trajectory groups" with the alcohol fraction, alkane fraction, carbonyl fraction, and OM/OC having ranges of 1–5%, 44–65%, 3–8%, and 1.29–1.49, respectively. Using these same measurements, Heald et al. (2005) calculated that OC concentrations were on average 4 $\mu g\,m^{-3}$ between 2 to 6.5 km (OM~5–6 $\mu g\,m^{-3}$). Since the focus of that study was on Asian pollution plumes in the proximity of their sources, the averages were probably heavily weighted to the high concentrations associated with recent emissions. Nevertheless, our upper limit of average OM concentrations for the Pacific air masses (4 $\mu g\,m^{-3}$) is similar to their average. Heald et al. (2005) also estimated a "free tropospheric background" of 1–3 $\mu g\,m^{-3}$ OC (OM~1.5–4$\mu g\,m^{-3}$) that was not associated with carbon monoxide or sulfate. The range of OM concentrations for the Pacific air masses (2.5–4 $\mu g\,m^{-3}$) is more consistent with that range.

Despite some small differences in the air mass regions we identified in this study, it is noteworthy that the variability of OM concentrations and alkane and alcohol fractions of OM within each region is broader than the differences in their means. Most trace element concentrations did not vary significantly within or among the different air mass categories. Similar variability is evident in an extensive compilation of global organic carbon measurements (Bahadur et al., 2009).

ACPD
9, 6657–6690, 2009

Only two of the Pacific or Continental samples for which we report organic composition were associated with strong pollution signatures (one Pacific and one Continental). Both were collected above 6000 m and were associated with elevated CO (280 ppb and 220 ppb), NO_y (1.2 ppb and 1.3 ppb), and O_3 (111 ppb and 97 ppb), concentrations much higher than typical free tropospheric or unpolluted boundary layer concentrations at this latitude. These samples were collected in air masses that Dunlea et al. (2008) identified in their case study as originating in East Asia 3–4 days earlier (using back trajectories from FLEXPART). However, since this campaign targeted Asian pollution, OM concentrations for the Pacific and Continental aloft air masses may be high compared to the regional average.

For the Continental air masses, the average degree of oxidation of organic aerosol (OM/OC=1.7–1.9) is similar to observations at locations affected by North American continental sources. Gilardoni et al. (2007) report average OM/OC ratios of ~1.4 for near-source airborne and 1.5–1.6 for coastal, ground-based measurements during the ICARTT 2004 study, conducted in the Northeastern US and Southeastern Canadian coastal region. OM/OC ratios over Mexico (Gilardoni et al., 2009) showed higher OM/OC ratios (average: 1.7–2.0), similar to that observed for our Continental average. In contrast to the Continental samples which showed a large variability in OM/OC (1.7±0.4), the observed OM/OC for the Central Valley samples was nearly constant (1.4±0.1). However, the OM concentrations in the Central Valley were higher and more variable, spanning a factor of five. This contrast in variability of OM concentrations and OM/OC in the Central Valley is analogous to other observations in which extrinsic aerosol properties (such as mass, light scattering, or absorption) showed a larger variability than aerosol size distributions or intrinsic properties (e.g. mass scattering efficiency, single scattering albedo) (Clarke et al., 2002; Quinn et al., 2004).

Emissions directly from combustion sources can be associated with large fractions of organic aerosol comprised of oxygenated functional groups (Russell et al., 2009). Russell et al. (2009) showed that oil and wood combustion emissions accounted for two-thirds of the OM in particles measured in Houston, and that direct emissions had

ACPD
9, 6657–6690, 2009

a significant O/C ratio, 0.30–0.33, approximately half that associated with the "processed" aerosol component.

It has been shown that the major component of SOA formation is due to biogenic VOC emissions, primarily emitted from forest ecosystems (Kanakidou et al., 2005). Temperate and boreal forests, over which some of the Continental air masses may have been transported, are known to emit large amounts of biogenic VOC (Tsigaridis et al., 2005; Spracklen et al., 2008). A significant fraction of SOA formation may occur in the free troposphere due to the lower temperatures favoring increased condensation (Tsigaridis and Kanakidou, 2003). Zhang et al. (2007) observe that more highly oxidized OM was more prevalent for urban influenced sites whereas less oxidized OM was correlated with biogenic OM.

5 Conclusions

OM concentrations were fairly variable within the different air mass categories (excluding Seattle) and did not show large differences among air mass averages, which were 2.2–4.5, 3.4–4.5, 2.6–3.9, and 1.4–3.1 $\mu g\,m^{-3}$ for the Continental, Central Valley, Pacific, and Seattle air masses, respectively. Alkane functional groups were the largest fraction of OM in all air masses. Alcohol functional group concentrations were highest for the Continental and Central Valley air masses and lowest for the Pacific and Seattle air masses. When detected, carboxylic acid functional groups comprised a large faction of OM (30–50%) in some Continental air masses. The degree of oxidation, reported as the OM/OC and O/C ratios, was observed to be more variable for Continental air masses compared to nearly constant values for the Central Valley, indicating a wider range of sources and processing controlling organic aerosol composition in the larger air mass region.

Samples were collected at a range of altitudes within the troposphere; however, there were few observable vertical trends. On average, OM was higher and more variable at lower altitudes, primarily due to the high values observed in the California

ACPD
9, 6657–6690, 2009

Central Valley. Otherwise, no consistent trends with altitude in OM, functional groups, functional group fractions, or O/C were apparent. Concentrations aloft of many of the trace metals were comparable to those measured aloft in Mexico. Most did not show any significant altitude dependence other than a few samples that were elevated in several trace metals associated with dust and also anthropogenic sources, possibly indicative of transport from the Asian continent. Sulfur was observed to decrease with altitude, consistent with marine or continental boundary layer sources.

Single particle analysis using STXM-NEXAFS showed that a large variety of particles from a mixture of different sources and processes were responsible for the organic particle composition in this region. Particles that may have resulted from secondary aerosol formation were the most common particle type observed, at a range of altitudes and regions. Combustion-type particles were also common. In addition, particles indicative of soil dust and also biomass burning were observed in several lower altitude samples. Quantitative analysis of absorbance ratios for STXM-NEXAFS spectra indicate that condensation and surface-limited oxidation processes may have been important growth processes for particles identified as Secondary.

Since our observations targeted a limited range of air mass types, more temporally and geographically extensive observations will be necessary to quantify the average concentrations of OM in the free troposphere over the Northeast Pacific. Many of the organic and elemental concentrations and organic particle types were similar to air mass regions in other studies (Maria et al., 2003; Gilardoni et al., 2007; Takahama et al., 2007; Gilardoni et al., 2009; Liu et al., 2009; Russell et al., 2009).

Acknowledgements. Grant support for this work was provided by NSF (ATM 05-11772). In addition we bn are grateful to Greg Kok, John Walker, Greg Roberts, and the NCAR C130 crew for valuable assistance during sample collection.

References

Ade, H. and Urquhart, S. G.: NEXAFS spectroscopy and microscopy of natural and synthetic polymers, in: Chemical Applications of Synchrotron Radiation, edited by: Sham, T. K. E., World Scientific Publishing, Singapore, 285–355, 2002. 6672

Aiken, A. C., Decarlo, P. F., Kroll, J. H., Worsnop, D. R., Huffman, J. A., Docherty, K. S., Ulbrich, I. M., Mohr, C., Kimmel, J. R., Sueper, D., Sun, Y., Zhang, Q., Trimborn, A., Northway, M., Ziemann, P. J., Canagaratna, M. R., Onasch, T. B., Alfarra, M. R., Prevot, A. S. H., Dommen, J., Duplissy, J., Metzger, A., Baltensperger, U., and Jimenez, J. L.: O/C and OM/OC ratios of primary, secondary, and ambient organic aerosols with high-resolution time-of-flight aerosol mass spectrometry, Environ. Sci. Technol., 42, 4478–4485, doi:10.1021/es703009q, 2008. 6662

Alfarra, M. R., Coe, H., Allan, J. D., Bower, K. N., Boudries, H., Canagaratna, M. R., Jimenez, J. L., Jayne, J. T., Garforth, A. A., Li, S. M., and Worsnop, D. R.: Characterization of urban and rural organic particulate in the lower Fraser valley using two aerodyne aerosol mass spectrometers, Atmos. Environ., 38, 5745–5758, doi:10.1016/j.atmosenv.2004.01.054, 2004. 6659

Bahadur, R., Gazala, H., and Russell, L. M.: Climatology of $PM_{2.5}$ organic carbon concentrations from a review of ground-based atmospheric measurements by evolved gas analysis, Atmos. Environ., 43, 1591–1602, 2009. 6674

Braun, A.: Carbon speciation in airborne particulate matter with C (1s) NEXAFS spectroscopy, J. Environ. Monitor., 7, 1059–1065, doi:10.1039/b508910g, 2005. 6671

Chung, S. H. and Seinfeld, J. H.: Global distribution and climate forcing of carbonaceous aerosols, J. Geophys. Res., 107, 4407, doi:10.1029/2001JD001397, 2002. 6659

Clarke, A. D., Howell, S., Quinn, P. K., Bates, T. S., Ogren, J. A., Andrews, E., Jefferson, A., Massling, A., Mayol-Bracero, O., Maring, H., Savoie, D., and Cass, G.: INDOEX aerosol: A comparison and summary of chemical, microphysical, and optical properties observed from land, ship, and aircraft, J. Geophys. Res., 107, 8033, doi:803310.1029/2001JD000572, 2002. 6675

Dibb, J. E., Talbot, R. W., Scheuer, E. M., Blake, D. R., Blake, N. J., Gregory, G. L., Sachse, G. W., and Thornton, D. C.: Aerosol chemical composition and distribution during the Pacific Exploratory Mission (PEM) Tropics, J. Geophys. Res., 104, 5785–5800, 1999. 6670

Dunlea, E. J., DeCarlo, P. F., Aiken, A. C., Kimmel, J. R., Peltier, R. E., Weber, R. J., Tomlison,

J., Collins, D. R., Shinozuka, Y., McNaughton, C. S., Howell, S. G., Clarke, A. D., Emmons, L. K., Apel, E. C., Pfister, G. G., van Donkelaar, A., Martin, R. V., Millet, D. B., Heald, C. L., and Jimenez, J. L.: Evolution of Asian aerosols during transpacific transport in INTEX-B, Atmos. Chem. Phys. Discuss., 8, 15375–15461, 2008, http://www.atmos-chem-phys-discuss.net/8/15375/2008/. 6662, 6664, 6665, 6667, 6669, 6670

Gilardoni, S., Russell, L. M., Sorooshian, A., Flagan, R. C., Seinfeld, J. H., Bates, T. S., Quinn, P. K., Allan, J. D., Williams, B., Goldstein, A. H., Onasch, T. B., and Worsnop, D. R.: Regional variation of organic functional groups in aerosol particles on four US east coast platforms during the International Consortium for Atmospheric Research on Transport and Transformation 2004 campaign, J. Geophys. Res., 112, D10S27, doi:10.1029/2006JD007737, 2007. 6661, 6674, 6675, 6677

Gilardoni, S., Shang, L., Takahama, S., Russell, L. M., Allan, J. D., Steinbrecher, R., Jimenez, J. L., Decarlo, P. F., Dunlea, E. J., and Baumgardner, D.: Characterization of organic ambient aerosol during MIRAGE 2006 on three platforms, Atmos. Chem. Phys. Discuss., 9, 6617–6655, 2009, http://www.atmos-chem-phys-discuss.net/9/6617/2009/. 6668, 6673, 6675, 6677

Heald, C. L., Jacob, D. J., Park, R. J., Russell, L. M., Huebert, B. J., Seinfeld, J. H., Liao, H., and Weber, R. J.: A large organic aerosol source in the free troposphere missing from current models, Geophys. Res. Lett., 32, L18809, doi:10.1029/2005GL023831, 2005. 6659, 6667, 6670, 6674

Johnson, K. S., de Foy, B., Zuberi, B., Molina, L. T., Molina, M. J., Xie, Y., Laskin, A., and Shutthanandan, V.: Aerosol composition and source apportionment in the Mexico City Metropolitan Area with PIXE/PESA/STIM and multivariate analysis, Atmos. Chem. Phys., 6, 4591–4600, 2006, http://www.atmos-chem-phys.net/6/4591/2006/. 6669

Johnson, K. S., Laskin, A., Jimenez, J. L., Shutthanandan, V., Molina, L. T., Salcedo, D., Dzepina, K., and Molina, M. J.: Comparative analysis of urban atmospheric aerosol by particle-induced X-ray emission (PIXE), proton elastic scattering analysis (PESA), and aerosol mass spectrometry (AMS), Environ. Sci. Technol., 42, 6619–6624, doi:10.1021/es800393e, 2008. 6668

Kanakidou, M., Seinfeld, J. H., Pandis, S. N., Barnes, I., Dentener, F. J., Facchini, M. C., Van Dingenen, R., Ervens, B., Nenes, A., Nielsen, C. J., Swietlicki, E., Putaud, J. P., Balkanski,

Y., Fuzzi, S., Horth, J., Moortgat, G. K., Winterhalter, R., Myhre, C. E. L., Tsigaridis, K., Vignati, E., Stephanou, E. G., and Wilson, J.: Organic aerosol and global climate modelling: a review, Atmos. Chem. Phys., 5, 1053–1123, 2005, http://www.atmos-chem-phys.net/5/1053/2005/. 6676

Leaitch, W. R., Macdonald, A. M., Anlauf, K. G., Liu, P. S. K., Toom-Sauntry, D., Li, S.-M., Liggio, J., Hayden, K., Wasey, M. A., Russell, L. M., Takahama, S., Liu, S., van Donkelaar, A., Duck, T., Martin, R. V., Zhang, Q., Sun, Y., McKendry, I., Shantz, N. C., and Cubison, M.: Evidence for Asian dust effects from aerosol plume measurements during INTEX-B 2006 near Whistler, BC, Atmos. Chem. Phys. Discuss., 8, 18531–18589, 2008, http://www.atmos-chem-phys-discuss.net/8/18531/2008/. 6672

Lewis, A. C., Carslaw, N., Marriott, P. J., Kinghorn, R. M., Morrison, P., Lee, A. L., Bartle, K. D., and Pilling, M. J.: A larger pool of ozone-forming carbon compounds in urban atmospheres, Nature, 405, 778–781, 2000. 6659

Liu, S., Takahama, S., Russell, L. M., Gilardoni, S., and Baumgardner, D.: Oxygenated organic functional groups and their sources in single and submicron organic particles in MILAGRO 2006 campaign, Atmos. Chem. Phys. Discuss., 9, 4567–4607, 2009, http://www.atmos-chem-phys-discuss.net/9/4567/2009/. 6661, 6668, 6677

Malm, W. C., Sisler, J. F., Huffman, D., Eldred, R. A., and Cahill, T. A.: Spatial and seasonal trends in particle concentration and optical extinction in the United States, J. Geophys. Res., 99, 1347–1370, 1994. 6669

Maria, S. F., Russell, L. M., Turpin, B. J., and Porcja, R. J.: FTIR measurements of functional groups and organic mass in aerosol samples over the Caribbean, Atmos. Environ., 36, 5185–5196, 2002. 6661

Maria, S. F., Russell, L. M., Turpin, B. J., Porcja, R. J., Campos, T. L., Weber, R. J., and Huebert, B. J.: Source signatures of carbon monoxide and organic functional groups in Asian Pacific Regional Aerosol Characterization Experiment (ACE-Asia) submicron aerosol types, J. Geophys. Res., 108, 8637, doi:10.1029/2003JD003703, 2003. 6661, 6663, 6669, 6674, 6677

Maria, S. F., Russell, L. M., Gilles, M. K., and Myneni, S. C. B.: Organic aerosol growth mechanisms and their climate-forcing implications, Science, 306, 1921–1924, doi:10.1126/science.1103491, 2004. 6664, 6673

McKendry, I. G., Macdonald, A. M., Leaitch, W. R., van Donkelaar, A., Zhang, Q., Duck, T., and Martin, R. V.: Trans-Pacific dust events observed at Whistler, British Columbia during

INTEX-B, Atmos. Chem. Phys., 8, 6297–6307, 2008, http://www.atmos-chem-phys.net/8/6297/2008/. 6669, 6670
Middlebrook, A. M., Murphy, D. M., and Thomson, D. S.: Observations of organic material in individual marine particles at Cape Grim during the First Aerosol Characterization Experiment (ACE 1), J. Geophys. Res., 103, 16475–16483, 1998. 6659
Miranda, J., Andrade, E., Lopez-Suarez, A., Ledesma, R., Cahill, T. A., and Wakabayashi, P. H.: A receptor model for atmospheric aerosols from a southwestern site in Mexico City, Atmos. Environ., 30, 3471–3479, 1996. 6668
Novakov, T., Hegg, D. A., and Hobbs, P. V.: Airborne measurements of carbonaceous aerosols on the East Coast of the United States, J. Geophys. Res., 102, 30023–30030, 1997. 6659
Peltier, R. E., Hecobian, A. H., Weber, R. J., Stohl, A., Atlas, E. L., Riemer, D. D., Blake, D. R., Apel, E., Campos, T., and Karl, T.: Investigating the sources and atmospheric processing of fine particles from Asia and the Northwestern United States measured during INTEX B, Atmos. Chem. Phys., 8, 1835–1853, 2008, http://www.atmos-chem-phys.net/8/1835/2008/.
Quinn, P. K., Coffman, D. J., Bates, T. S., Welton, E. J., Covert, D. S., Miller, T. L., Johnson, J. E., Maria, S., Russell, L., Arimoto, R., Carrico, C. M., Rood, M. J., and Anderson, J.: Aerosol optical properties measured on board the Ronald H. Brown during ACE-Asia as a function of aerosol chemical composition and source region, J. Geophys. Res., 109, D19S01, doi:10.1029/2003JD004010, 2004. 6675
Russell, L. M., Maria, S. F., and Myneni, S. C. B.: Mapping organic coatings on atmospheric particles, Geophys. Res. Lett., 29, 1779, doi:10.1029/2002GL014874, 2002. 6663
Russell, L. M., Takahama, S., Liu, S., Hawkins, L. N., Covert, D. S., Quinn, P. K., and Bates, T. S.: Oxygenated fraction and mass of organic aerosol from direct emission and atmospheric processing collected on the R/V Ronald Brown during TEXAQS/GoMACCS 2006, J. Geophys. Res.-A, in press, online available at: http://www.agu.org/contents/journals/ViewPapersInPress.do?journalCode=JD#id2008JD011275, 2009. 6661, 6668, 6675, 6677
Singh, H. B., Brune, W. H., Crawford, J. H., Flocke, F., and Jacob, D. J.: Chemistry and transport of pollution over the Gulf of Mexico and the Pacific: Spring 2006 INTEX-B Campaign overview and first results, Atmos. Chem. Phys. Discuss., 9, 363–409, 2009, http://www.atmos-chem-phys-discuss.net/9/363/2009/. 6659
Spracklen, D. V., Bonn, B., and Carslaw, K. S.: Boreal forests, aerosols and the impacts on clouds and climate, Philos. Tr. R. Soc. S.-A, 366, 4613–4626, doi:10.1098/rsta.2008.0201,

2008. 6676

Takahama, S., Gilardoni, S., Russell, L. M., and Kilcoyne, A. L. D.: Classification of multiple types of organic carbon composition in atmospheric particles by scanning transmission X-ray microscopy analysis, Atmos. Environ., 41, 9435–9451, doi:10.1016/j.atmosenv.2007.08.051, 2007. 6663, 6664, 6671, 6672, 6677, 6688

Tsigaridis, K. and Kanakidou, M.: Global modelling of secondary organic aerosol in the troposphere: a sensitivity analysis, Atmos. Chem. Phys., 3, 1849–1869, 2003, http://www.atmos-chem-phys.net/3/1849/2003/. 6676

Tsigaridis, K., Lathiére, J., Kanakidou, M., and Hauglustaine, D. A.: Naturally driven variability in the global secondary organic aerosol over a decade, Atmos. Chem. Phys., 5, 1891–1904, 2005, http://www.atmos-chem-phys.net/5/1891/2005/. 6676

Turpin, B. J. and Lim, H. J.: Species contributions to $PM_{2.5}$ mass concentrations: Revisiting common assumptions for estimating organic mass, Aerosol Sci. Technol., 35, 602–610, 2001. 6659

Zhang, Q., Canagaratna, M. R., Jayne, J. T., Worsnop, D. R. and Jimenez, J. L.: Time- and size-resolved chemical composition of submicron particles in Pittsburgh: Implications for aerosol sources and processes, J. Geophys. Res., 110, D07S09, doi:10.1029/2004JD004649, 2005. 6659

Zhang, Q., Jimenez, J. L., Canagaratna, M. R., Allan, J. D., Coe, H., Ulbrich, I., Alfarra, M. R., Takami, A., Middlebrook, A. M., Sun, Y. L., Dzepina, K., Dunlea, E., Docherty, K., DeCarlo, P. F., Salcedo, D., Onasch, T., Jayne, J. T., Miyoshi, T., Shimono, A., Hatakeyama, S., Takegawa, N., Kondo, Y., Schneider, J., Drewnick, F., Borrmann, S., Weimer, S., Demerjian, K., Williams, P., Bower, K., Bahreini, R., Cottrell, L., Griffin, R. J., Rautiainen, J., Sun, J. Y., Zhang, Y. M., and Worsnop, D. R.: Ubiquity and dominance of oxygenated species in organic aerosols in anthropogenically-influenced Northern Hemisphere midlatitudes, Geophys. Res. Lett., 34, L13801, doi:10.1029/2007GL029979, 2007. 6676

Table 1. OM concentrations, organic functional group concentrations and fraction of OM, O/C and OM/OC ratios, and elemental concentrations for Continental, Central Valley, Pacific, and Seattle air mass sectors and campaign averages ("INTEX-B") measured by FTIR and XRF. Ranges are shown for the FTIR measurements and indicate the means of the measurements and the upper limit bounds. XRF concentrations are expressed as means and standard deviations of the measurements.

		Continental	Central Valley	Pacific	Seattle	INTEX-B
	FTIR OM ($\mu g\,m^{-3}$)	2.2–4.5	3.4–4.5	2.6–3.9	1.4–3.1	2.4–4.1
	FTIR OM/OC	1.7–1.9	1.4–1.7	–	–	1.6–1.8
	FTIR O/C	0.4–0.6	0.2–0.4	–	–	0.3–0.5
FTIR Organic Functional Groups ($\mu g\,m^{-3}$)	Alcohol	0.46–0.51	0.49–0.49	0.16–0.24	0.16–0.24	0.35–0.39
	Alkane	1.4–1.9	2.5–2.5	2.4–2.4	1.2–1.3	1.9–2.1
	Carboxylic Acid	0.4–2.0	0.4–1.5	0–1.3	0.04–1.5	0.2–1.6
XRF Elements ($ng\,m^{-3}$)	Na	490±300	–	–	416±0	460±220
	Al	200±170	120±82	190±190	120±43	170±150
	Si	210±170	170±80	280±250	200±56	230±180
	S	210±100	420±110	240±220	250±110	250±170
	Cl	56±15	74±0	81±25	–	67±19
	K	34±16	110±90	49±25	39±17	47±35
	Ca	82±44	30±11	51±27	140±170	76±81
	V	29±21	14±11	32±29	14±9	25±21
	Fe	47±20	24±5	50±26	69±19	48±23
	Ni	46±18	27±0	51±43	–	47±31
	Cu	28±0	–	32±24	–	31±17
	Zn	51±27	17±12	50±44	46±0	44±31
	As	16±0	–	15±0	8±0	13±4
	Sn	250±230	98±96	260±260	130±88	210±210
	Ba	67±54	21±0	86±74	23±0	71±64
	Hg	25±0	–	25±16	–	25±12

ACPD
9, 6657–6690, 2009

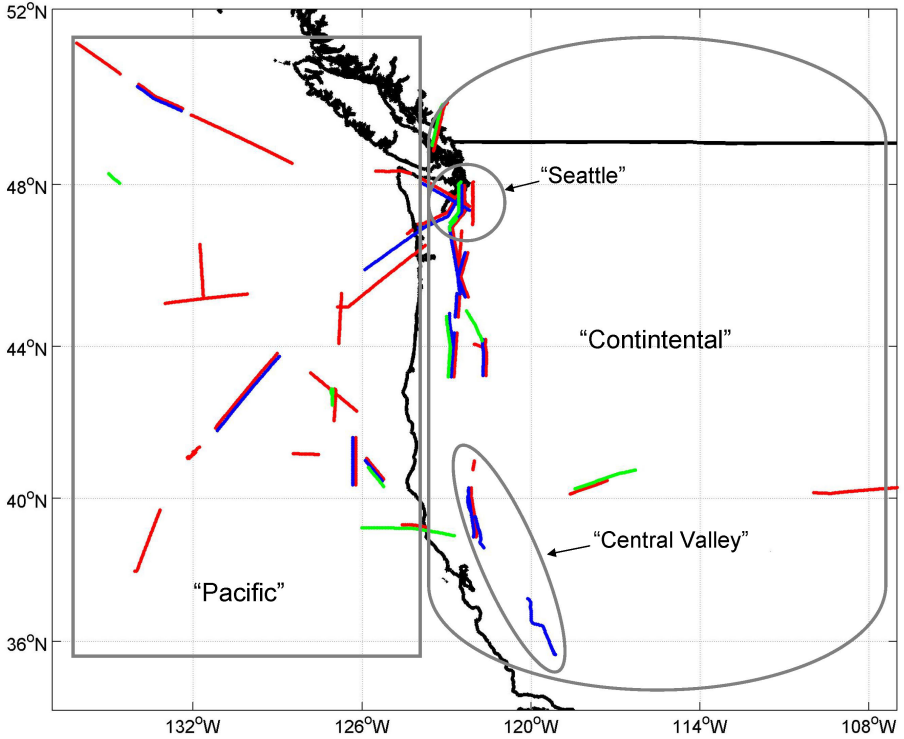

Fig. 1. Map showing the locations of all the reported (constant altitude) samples with the analytical method indicated (red=XRF, blue=FTIR, green=STXM). Overlapping tracks are slightly offset to show all tracks. Grey lines encompass the four air mass regions.

ACPD
9, 6657–6690, 2009

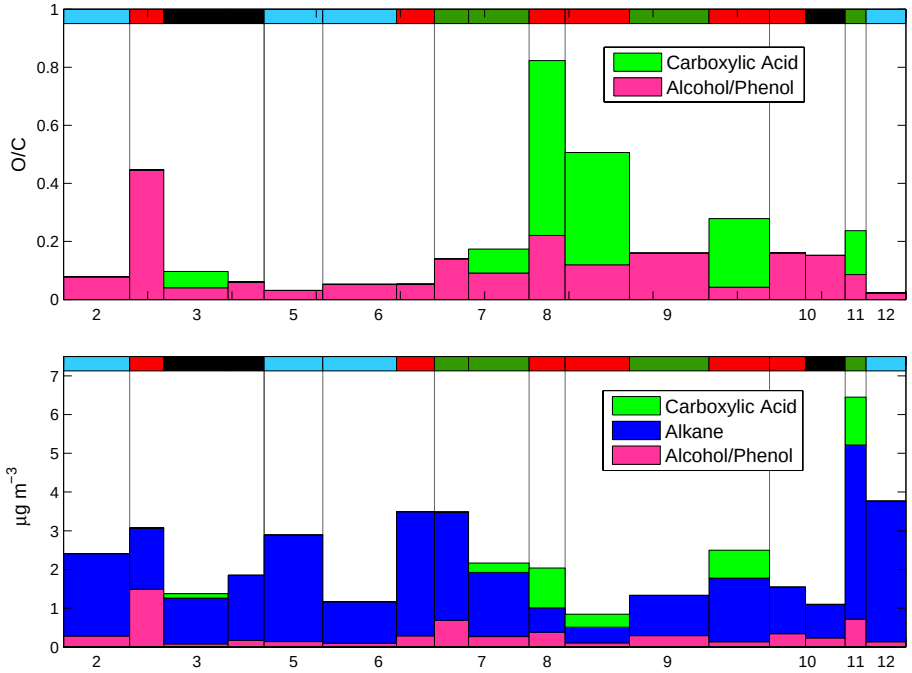

Fig. 2. Organic functional group concentrations and O/C contributions grouped by research flight: alcohol (pink), alkane (blue), and carboxylic acid (light green). Bar widths are proportional to sampling time. Air mass categories are indicated by color bars at the top: Central Valley (dark green), Continental (red), Pacific (light blue), and Seattle (black).

ACPD
9, 6657–6690, 2009

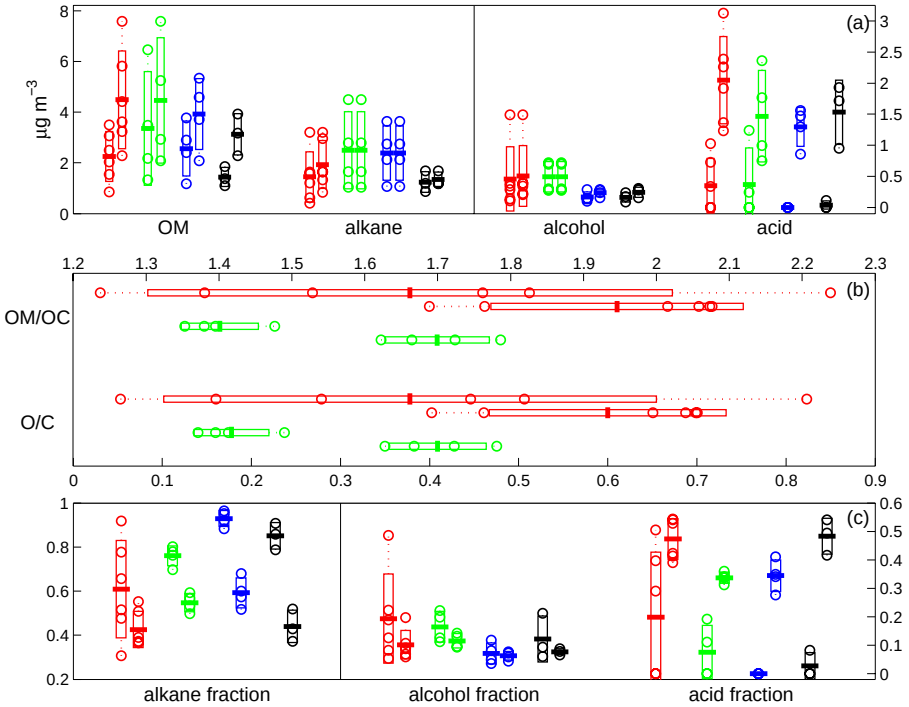

Fig. 3. (a) Organic functional group concentrations (μg m^{-3}); **(b)** OM/OC ratios and O/C ratios; and **(c)** organic functional group fractions of the total OM. The measurements (circles) have been overlaid with dark bars that indicate the mean value and boxes that indicate the standard deviation. Whiskers specify grouping of measurements not contained within boxes. The bars and boxes are meant as a rough visual guide rather than a robust statistical measure. The observations are separated into the four air mass categories: Continental (red), Central Valley (green), Pacific (blue), and Seattle (black). For each air mass, a pair is shown representing the measurements on the left and the upper bounds on the right.

ACPD
9, 6657–6690, 2009

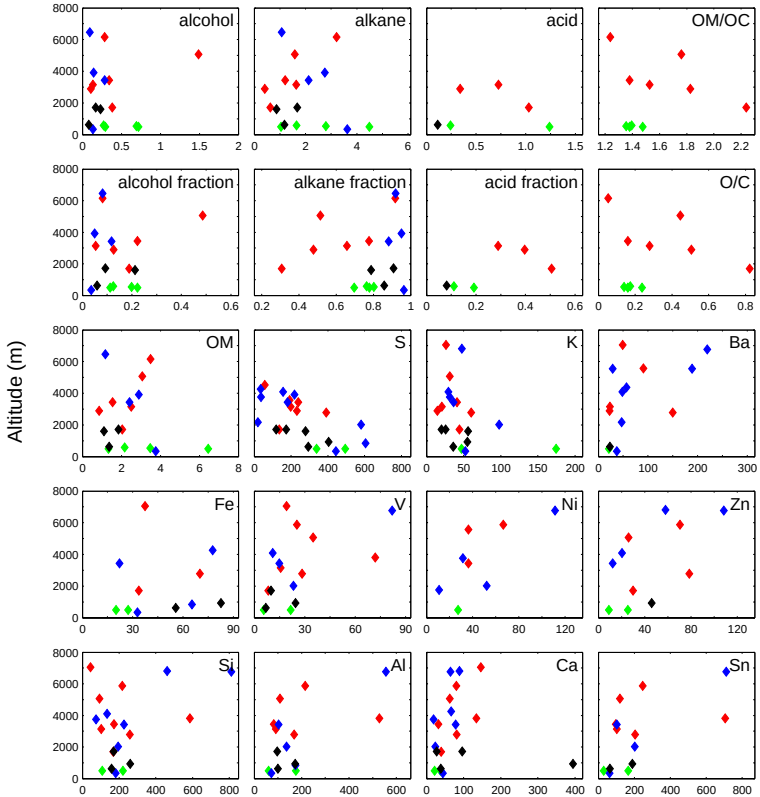

Fig. 4. Organic functional group concentrations ($\mu g\,m^{-3}$), fractions of OM, OM/OC and O/C ratios, and trace element concentrations ($ng\,m^{-3}$) as a function of altitude. Air mass categories are designated by color: Central Valley (green), Continental (red), Pacific (blue), and Seattle (black).

ACPD
9, 6657–6690, 2009

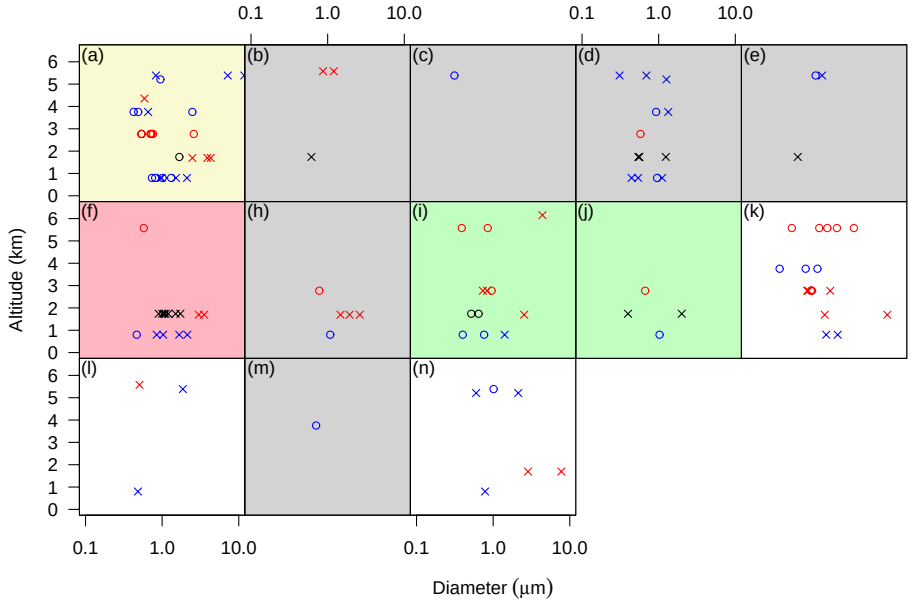

Fig. 5. Summary of particles analyzed by STXM-NEXAFS. Panels represent previously established categories (Takahama et al., 2007); average spectrum of each particle type is used for classification into these groups. Shaded panels indicate metaclasses: Combustion (grey), Ultisol (light red), Secondary (light yellow), and Biomass (light green). (x) indicates irregular particle and (o) indicates spherical particle. Symbol colors indicate air mass categories: Continental (red), Pacific (blue), and Seattle (black).

ACPD
9, 6657–6690, 2009

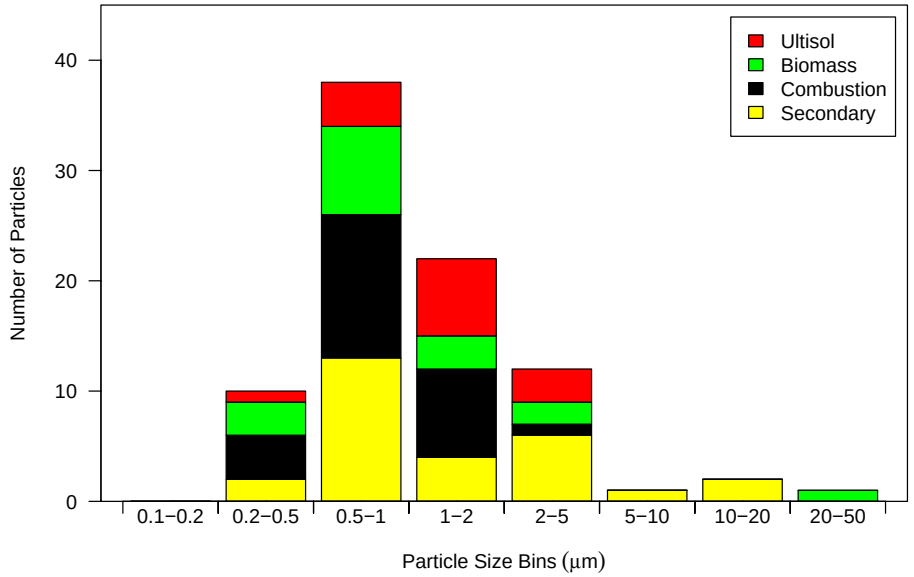

Fig. 6. Histogram of size and metaclass of particles analyzed by STXM-NEXAFS. Metaclasses are indicated by darker shades corresponding to Fig. 5: Combustion (black), Ultisol (red), Secondary (yellow), and Biomass (green).

ACPD
9, 6657–6690, 2009

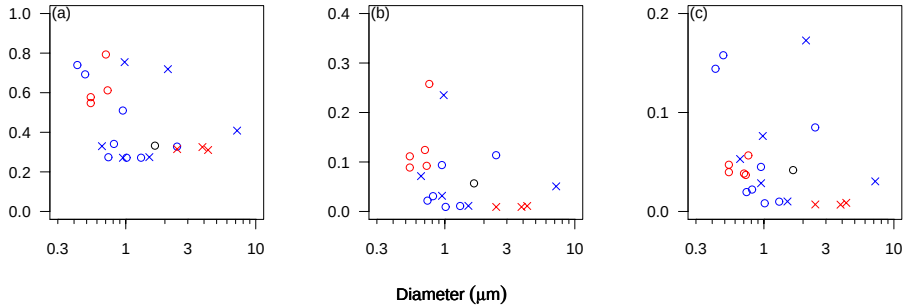

Fig. 7. Absorbance ratios plotted as a function of particle diameter from the quantitative analysis of STXM-NEXAFS spectra identified as Secondary: **(a)** total carbon-to-total mass ratio; **(b)** carboxylic carbonyl carbon-to-total mass ratio; **(c)** carboxylic carbonyl carbon-to-carbon ratio. (x) indicates irregular particle and (o) indicates spherical particle. Symbol colors indicate air mass categories: Continental (red), Pacific (blue), and Seattle (black).

ACPD
9, 6657–6690, 2009